Interaction of small gold clusters with carbon nanotube bundles: formation of gold atomic

chains

Interaction of small gold clusters with carbon nanotube bundles: formation of gold atomic chains

J Deepak[1], T Pradeep[1] and U V Waghmare[2]

[1] Indian Institute of Technology Madras, Chennai 600 036, India
[2] JNCASR, Jakkur, Bangalore 560 064, India

Abstract
We use first-principles density functional theory to simulate the interaction of bundles of semiconducting (10, 0) and metallic (6, 6) carbon nanotubes (CNTs) with small gold clusters (Au_n, $n = 3, 5$) inserted in their interstitial spaces. We find that gold clusters spontaneously evolve to form atomic chains along the axis of nanotubes and induce weak metallicity in the semiconducting nanotubes through charge transfer. We further show that a similar structural evolution of Pt_3 clusters occurs in the interstitial spaces of a (10, 0) CNT bundle. Our calculations show that these structural changes, along with interesting changes in the electronic structure, occur at moderate pressures that are readily achievable in a laboratory, and should be relevant to devices that make use of gold–nanotube contacts.

(Some figures in this article are in colour only in the electronic version)

Carbon nanotubes (CNT) are one-dimensional nanostructures with potential applications in diverse fields of nanoelectronics, catalysis, chemical sensing and hydrogen storage devices [1–5]. The inherent properties of CNTs, such as extraordinary mechanical stiffness, geometry-dependent electrical conductivity and high surface area, are central to their diverse set of applications. The interaction of CNTs with surroundings, such as electrodes, clusters, molecules and liquids, is fundamentally interesting and plays an important role in their applications.

The coupling between CNTs and nanoparticles, molecules and external fields can be utilized to tailor the properties of CNTs for different applications. Functionalization of CNTs has been used to produce nanocomposites with enhanced physical properties [6–9]. Metal–nanotube hybrids have been investigated for their applicability in fuel cells, biological sensing and nanosized electronic devices [10]. Gold nanoparticles are commonly used to decorate sidewalls of single-walled carbon nanotubes (SWNTs) because of their biocompatibility and surface optical properties [11].

The interaction of CNTs with atoms and small clusters is also crucial to understanding how CNTs can be used as templates to grow novel nanostructures [12]. For example, attaching metal nanoparticles to CNT sidewalls leads to the synthesis of metal nanowires on CNT templates [13–16]. The

sidewalls of nanotubes have been coated with metal atoms to obtain metallic or superconducting nanowires [15, 16]. Formation of metallic nanowires on CNT sidewalls has been analysed in terms of the interaction between CNT and metal atoms [17, 18]. Strongly interacting metals like Ti, Ni and Pd were found to form nanowires while weakly interacting metals like Au, Al and Fe were found to form discontinuous particles decorating SWNT sidewalls [17]. Earlier, Charlier *et al* [19] investigated the interaction of gold clusters with an isolated CNT. Here, we investigate how the behaviour of the clusters changes when confined in a one-dimensional channel provided by the interstices in a CNT bundle. The finding of [19] of a weak interaction of gold clusters with a CNT is useful in understanding our results. CNTs, as synthesized, are often in the form of bundles and a large fraction of the surface area of nanotubes is exposed to the interstitial region of the bundle. Small metal clusters can be accommodated inside these confined spaces and their interaction with CNTs is fundamentally interesting and relevant to metal contacts with CNT bundles that are essential to many applications.

While important qualitative information can be extracted using spectroscopic methods and electron microscopy [20], experimental control over, and characterization of, the interface between nanotubes and nanoparticles is challenging, and a systematic theoretical investigation serves as a valuable
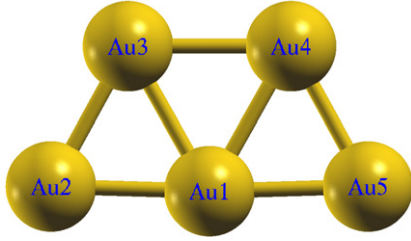
1

Figure 1. Isolated Au_5 cluster.

Table 1. Bond lengths and bond angles in Au_5 cluster.

Parameter	Current study	Reference [26]
d_{1-2} (Å)	2.64	2.64
d_{1-3} (Å)	2.77	2.78
α_{213} (deg)	58.9	59.6
α_{314} (deg)	58.9	58.0

Table 2. Diameter (D), periodicity (H) and lattice constant (a) in the direction perpendicular to the bundle axis.

SWNT bundle	D (Å)	H (Å)	a (Å)
(10, 0)	7.90	4.26	11.87
(6, 6)	8.14	2.46	11.92

complementary study. In this paper, we use first-principles calculations to simulate small gold clusters intercalated in the interstitial spaces in bundles of semiconducting and metallic CNTs. In a related work, Bendiab *et al* [21] have shown that Rb dopant atoms prefer to occupy the interstitial sites of CNT bundles only at concentrations below a certain stoichiometric limit and, with increasing concentration, the interior of the nanotubes and external surfaces become energetically more favourable in that order. We note that this limit may not be directly applicable to our study because of two reasons: (1) gold atoms are much smaller than Rb atoms and (2) nanotube diameters and interstitial channel sizes in our study are different (smaller diameters and wider interstitial channels). The stoichiometries we use roughly correspond to the limit described in [21] for interstitial site occupation multiplied by the size factor (size of Au/size of Rb) and hence in principle the interstitial site should be energetically favourable over other possible sites. We find that gold clusters confined in the sub-nanometre-sized spaces of CNT bundles transform spontaneously to one-dimensional atomic chains, undergoing large changes in their bonding through interaction with surrounding CNTs.

Our first-principles calculations are based on density functional theory as implemented in the quantum-espresso package [22], with the use of plane wave basis and pseudopotentials. We use a generalized gradient approximation (GGA) to the exchange–correlation energy functional as parametrized by Perdew, Burke and Ernzerhof (PBE) [23] and ultrasoft pseudopotentials [24] to model the interaction between core ion and valence electrons. We use a plane wave basis truncated at an energy cutoff of 25 Ryd to represent Kohn–Sham wavefunctions and that at 150 Ryd to represent the charge density. Structural optimization is carried out using the Broyden–Fletcher–Goldfarb–Shanno (BFGS) algorithm until the Hellman–Feynman forces are less than 0.001 Ryd /bohr.

To simulate gold clusters (Au_3 and Au_5), we use a supercell of large size (20 Å) to have negligible interactions between periodic images of clusters. Relaxed structures of isolated gold clusters Au_n ($n = 3, 5$) (see figure 1, table 1) agree reasonably well with those obtained by Hakkinen *et al* [26] through a very similar simulation methodology (PBE-GGA-based DFT).

To simulate bundles of SWNTs, we use a hexagonal periodic lattice with one CNT per cell. This has the periodicity of SWNTs along the axis (*c* axis) and its size in the *ab* plane is obtained through energy minimization. We find *a*—the lattice parameter (see table 2)—to be close to 11.9 Å for bundles of

both semiconducting (10, 0) and metallic (6, 6) CNTs. This is slightly larger than the LDA estimate of 11.4 Å for bundles of (6, 6) nanotubes [27], which is typical of LDA and GGA calculations. Our estimate of C–C bond length is 1.42 Å, in good agreement with earlier works [5].

The CNT bundle is simulated with a hexagonal lattice with one CNT per unit cell and a metal cluster placed in one of the two interstitial regions. To simulate an Au cluster intercalated in the CNT bundles, we use supercells of SWNT bundles obtained by multiplying unit cells along the bundle axis: a doubled unit cell for (10, 0) and a quadrupled unit cell for (6, 6) CNT bundles. Gold clusters Au_n ($n \geqslant 8$) are non-planar and cannot be accommodated in the voids of the SWNT bundle [26]. Size and symmetry of Au_7 and Au_6 do not permit insertion of these clusters in the interstitial spaces of a bundle with the supercells used here and Au_5 was a suitable candidate with the largest size. We use relaxed structures of gold clusters (both Au_3 and Au_5 are planar) and generated initial structures of the Au–CNT composites by locating the Au clusters in the interstitial space of the bundle with their plane perpendicular to the axis of CNTs. Structural optimization was carried out with several such choices of the initial structure to determine the most stable structure. We use a $1 \times 1 \times 30$ Monkhorst–Pack [25] mesh of *k*-points for sampling the Brillouin zone integration.

Upon relaxation, gold clusters in the (10, 0) bundle–Au composite evolve into chains of gold atoms in the interstitial space between the nanotubes (figure 2). In spite of being separated widely in the initial structures, gold atoms reassemble spontaneously to form the chain-like structure, meaning there is no energy barrier for this evolution. With marked changes in bond lengths and geometry with respect to the isolated cluster (table 3), the shortest distance between a carbon atom in the CNT and a gold atom increases from 1.3 to 2.29 Å. We note that diagonal and shear stresses on the supercell are all less than 20 kbar, suggesting that such structural evolution can occur under laboratory conditions; CNTs deform slightly due to these stress fields, as evident in a slightly elliptical shape (see figure 2).

On intercalation with gold clusters, a semiconducting (10, 0) CNT bundle becomes metallic (see figures 3(a) and (b)), which should not be surprising as there is the presence of a chain of gold atoms in the structure. From partial
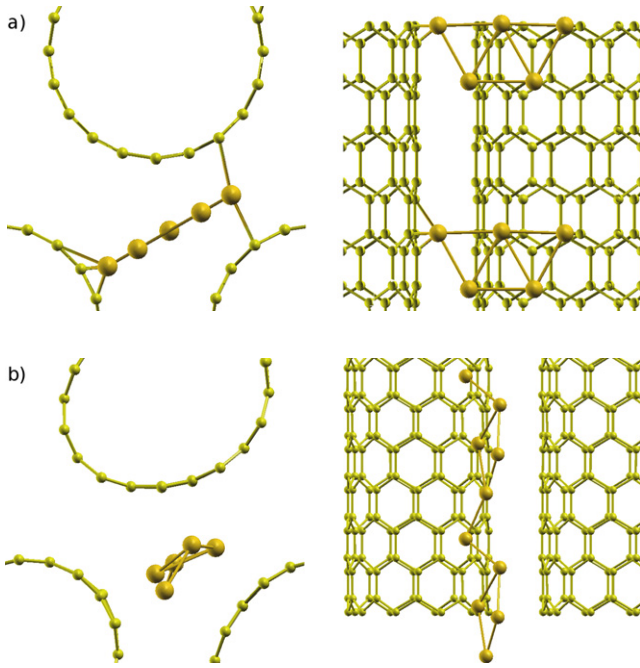
Figure 2. (10, 0) bundle–Au$_5$ composite: top and side views.
(a) Before and (b) after relaxation. Colour code (online): yellow—C,
gold—Au. The larger atoms are gold atoms.

Table 3. Structural parameters of Au$_5$ before and after relaxation in a
(10, 0) bundle. Notation: d—distance, α—angle, ϕ—dihedral angle.

Property	Isolated	Composite
d_{12} (Å)	2.64	2.80
d_{23} (Å)	2.67	3.67
d_{24} (Å)	4.64	2.76
d_{25} (Å)	5.29	2.66
α_{215} (deg)	180	57.7
α_{245} (deg)	88.5	57.3
ϕ_{1243} (deg)	180	160.6

possible origin of metallicity of the bundle, we determined
the electronic structure of a (10, 0) SWNT bundle, in the
deformed condition as obtained in the optimized structure of
the composite (figure 3(c)). We find the bundle to be still
semiconducting. We note a single (almost isolated) band
crossing the Fermi level (see the band structure in figure 3(a))
of the composite, which is responsible for the metallicity of
the composite. Visualization of the charge density isosurface
associated with a wavefunction in this particular band (see
figure 3(d)) demonstrates clearly the delocalized electronic
density at both CNT and Au atoms. Therefore, we infer that
metallicity of the SWNT bundle is due to charge transfer from
gold atoms to CNTs, similar to what has been found previously
in the context of K-doped SWNT bundles [28].

In order to further affirm the phenomenon of chain
formation, we repeated such a simulation with an Au$_3$ cluster,
but with a single unit cell of an SWNT bundle. Although the
cluster and its images were initially separated by 4.26 Å, it

density of states (DoS), we find, however, that the SWNT
bundle makes a nonzero contribution to DoS at the Fermi
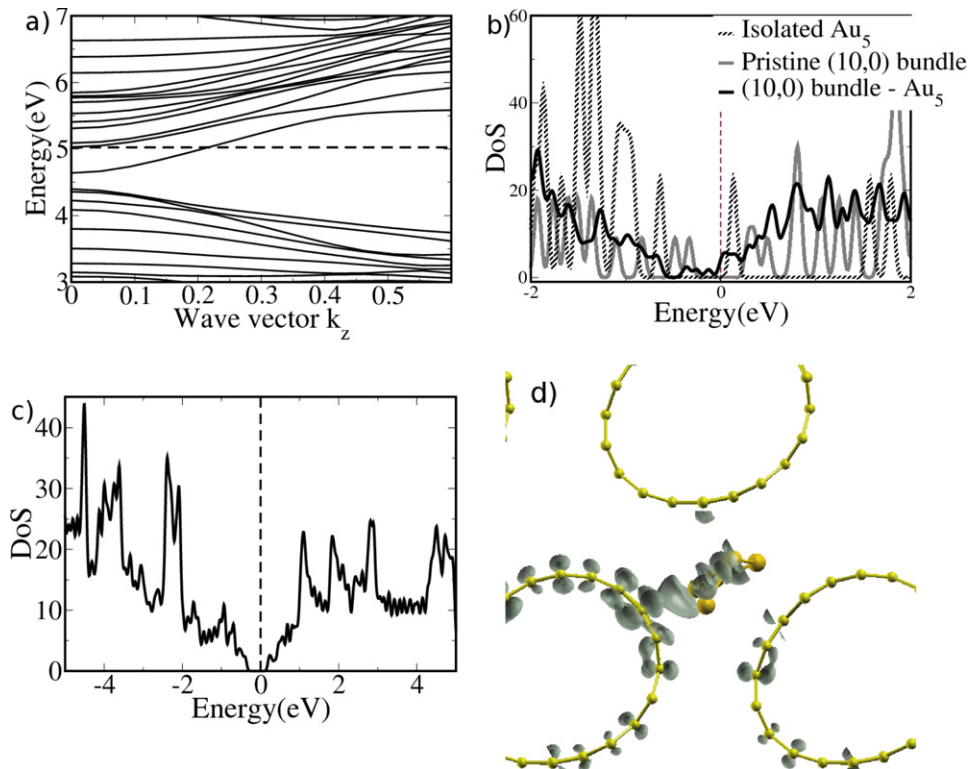level. In order to eliminate mechanical deformation as a

Figure 3. (a) Band structure of (10, 0) bundle–Au composite (Fermi level shown as a dashed line), (b) corresponding density of states (Fermi
level shifted to 0 eV), (c) DoS of mechanically deformed tube, (d) electron density isosurface of the band crossing the Fermi level in (a) at
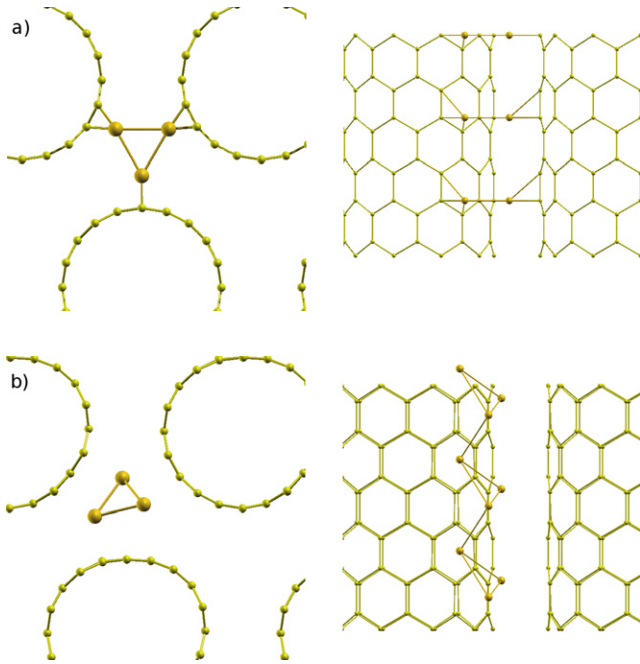12.5% of the maximum isovalue.

Figure 4. (10, 0) bundle intercalated with Au_3: top and side views. (a) Before and (b) after structural relaxation. Colour code (online): yellow—C, gold—Au. The larger atoms are gold atoms.

Figure 5. (6, 6) bundle intercalated with Au_5: top and side views. (a) Before and (b) after structural relaxation. Colour code (online): yellow—C, gold—Au. The larger atoms are gold atoms.
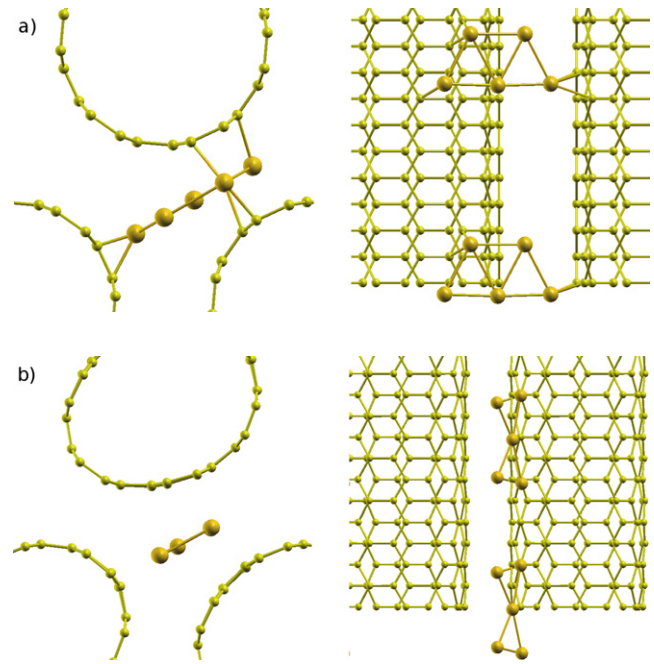
Table 4. Structural parameters of Au_5 before and after relaxation in a (6, 6) bundle. Notation: d—distance, α—angle.

Property	Initial	Relaxed
$d(Au_1–Au_2)$ (Å)	2.80	2.71
$d(Au_1–Au_3)$ (Å)	2.67	2.79
$\alpha(2–1–3)$ (deg)	58.6	58.0
$\alpha(3–1–4)$ (deg)	58.8	102.4

Figure 6. Density of states: (6, 6) SWNT bundle intercalated with Au_5. Fermi level has been shifted to 0 eV.

evolves upon relaxation to a chain structure, as in the case of an Au_5 cluster, thus confirming the tendency of gold clusters to transform into a chain of gold atoms (figure 4). The nearest distance between Au and C atoms is 2.3 Å, about the same as in the case of Au_5. The common feature in these simulations is that the chains lie at the centroid of the triangular interstitial space of the bundle. The stresses were found to be less than about 5 kbar in this case too.

Our simulations of Au_5 clusters intercalated in the (6, 6) bundle do not reveal any formation of Au chains in its interstices (see figure 5). The structure of Au_5 remains planar, though there are significant changes in bond lengths (see table 4). The nearest distance between gold and carbon atoms was found to be 2.29 Å, similar to that in the (10, 0) bundle. The fact that the cluster still remains planar is consistent with the fact that the interstitial space in the (6, 6) bundle is larger than that in the (10, 0) bundle.

To understand why chains do not form in the (6, 6) bundle, we analyse the geometry of the system. Gold–gold bond lengths estimated by electron microscopy in gold nanochains [29] are as long as 4 Å. Our simulations show that these bond lengths are much smaller when the Au chains are surrounded by CNTs (∼2.7 Å). Assuming an average
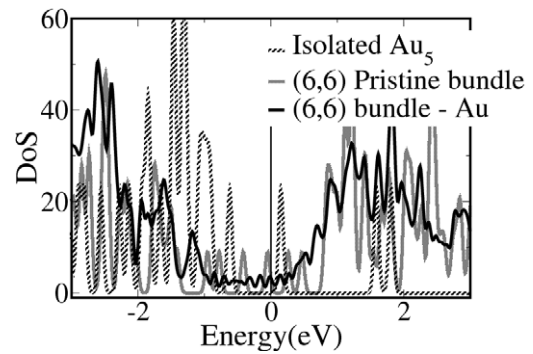
bond length of 2.7 Å, an overestimate of the minimum number of gold atoms required to form a chain would be 0.37 Å^{-1}. In our calculations of a (6, 6) bundle with five atoms of gold in a length of 9.84 Å (four times the periodicity of the (6, 6) bundle), this is equivalent to having 0.51 atoms Å^{-1}. Thus, although chain formation is allowed within geometric constraints, Au_5 units remain discrete in a (6, 6) bundle. As the stresses in the (6, 6) bundle–Au composite are all less than 10 kbar, such structures are feasible in laboratory conditions. A metallic (6, 6) bundle remains metallic upon insertion of Au clusters and does not show any significant changes in electronic structure (figure 6), in contrast to the (10, 0) bundle.

In order to examine if the absence of chain formation in the above simulation is a result of the relatively larger separation between the periodic images of Au_5 along the bundle axis, we repeated the simulation with an Au_3 cluster but with two unit cells of the (6, 6) SWNT bundle. Indeed, Au_3 clusters initially
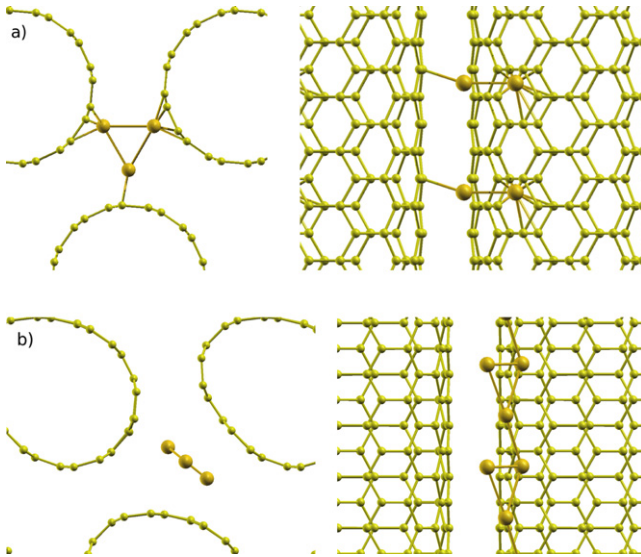
Figure 7. (6, 6) bundle intercalated with Au$_3$: top and side views. (a) Before and (b) after structural relaxation. Colour code: yellow—C, gold—Au.

separated by 4.52 Å (two times the periodicity of the (6, 6) bundle) strikingly evolved to form a continuous chain of gold atoms (figures 7(a) and (b)). This suggests that chain formation is a universal phenomenon in all SWNT bundles, irrespective of whether the bundle is semiconducting or metallic. The nearest distance between Au and C atoms is 2.3 Å, which is a common feature in all our simulations. The stresses were found to be less than 20 kbar, once again indicating that such structures can be realized under lab conditions.

To quantify the stability of the SWNT bundle–Au composite, we calculated the expression

$$S = \frac{E_{\text{composite}} - E_{\text{bundle}} - E_{\text{cluster}}}{\text{Number of gold atoms}} \quad (1)$$

where E indicates energy (table 5). The absolute values of S were all less than 0.4 eV/atom, slightly positive for composites formed from the Au$_5$ cluster and slightly negative for those formed from the Au$_3$ cluster. This can be explained by noting that in both the composites involving the Au$_3$ cluster, the structure adopted by the gold atoms upon relaxation is very similar to that in an isolated cluster (planar triangle), while in composites formed from an Au$_5$ cluster, the gold atoms undergo elaborate changes before continuous chain structure is achieved.

Lastly, we explored the possibility of chain formation with other metal clusters by performing calculations with a Pt$_3$ cluster in the interstices of a (10, 0) CNT. The bond length in equilateral triangle-shaped Pt$_3$ was found to be 2.49 Å, in agreement with the value obtained elsewhere [30] using a Perdew–Wang functional [31]. Using our earlier calculation with an Au$_3$ cluster in a (10, 0) CNT bundle as a template, we formed two structures, one based on the guessed structure having a Pt$_3$ cluster and its images separated and the other one similar to the relaxed structure having continuous chains of platinum atoms. The latter structure was found to be more

Table 5. Stability of SWNT–Au composite with respect to a mixture of SWNT bundles and clusters. S is defined in equation (1).

Composite	S (eV/atom)
(10, 0)–Au$_5$	0.29
(10, 0)–Au$_3$	−0.21
(6, 6)–Au$_5$	0.39
(6, 6)–Au$_3$	−0.18

stable than the former by more than 15 eV. Earlier studies on platinum chains using GGA report a maximum bond length of 2.9 Å [32]. Pt–Pt bond lengths in the chain structure ranged between 2.6 and 2.75 Å and are hence acceptable. The stresses were calculated to be less than 5 kbar. This suggests that Pt chains and, in general, metal chains could in principle be formed in the interstices of CNT bundles.

To summarize, our first-principles calculations on gold cluster intercalated SWNT bundles clearly demonstrate spontaneous evolution of Au$_5$ and Au$_3$ clusters into chain-like structures, which are guided by the surrounding three CNTs in the bundle. Interestingly, this behaviour seems to be more readily possible in semiconducting CNT bundles and results in weak metallicity in the CNT bundles. However, this does not seem to occur with non-planar clusters of gold, which are hard to be accommodated in the interstices of a CNT bundle. In principle, this method of formation of atomic chains seems to be more general, as suggested by our calculations with a Pt$_3$ cluster. The distance between periodic images (in the *ab* plane) of the clusters is large and their interactions are expected to be weak. However, gold clusters do interact with periodic images along the *c* axis in the interstitial channel, and variation in their density along the channel will result in discontinuities (in the low density region) in the otherwise continuous gold chain. This is indeed relevant to experiments, in using a combination of both theory and experiments, Charlier *et al* [19] have recently demonstrated that the spatial distribution of gold nanoparticles on individual nanotubes can be controlled by introducing structural and chemical defects on the nanotube surface which act as nucleation centres for nanoparticles. Recently, Meunier *et al* have demonstrated that Mo forms stable nanowires inside multi-walled carbon nanotubes [33]. Our work suggests another method to grow nanowires using carbon nanotube bundles, and is directly relevant to the science of contacts between gold and CNT bundles, which are essential components for any devices based on CNT bundles.

Acknowledgments

References

[1] Baughman R H, Zakhidov A A and de Heer W A 2002 *Science* **297** 787
[2] McEuen P L 1998 *Nature* **393** 15
[3] Kong J *et al* 2000 *Science* **287** 622

[4] Dillon A C *et al* 1997 *Nature* **386** 377
[5] Dresselhaus M, Dresselhaus G and Avouris Ph 2001 *Carbon Nanotubes: Synthesis, Structure, Properties and Applications* (Berlin: Springer)
[6] Dai H *et al* 1999 *J. Phys. Chem.* B **103** 11246
[7] Chen P *et al* 1999 *Science* **285** 91
[8] Planeix J M *et al* 1994 *J. Am. Chem. Soc.* **116** 7935
Qu L and Dai L 2005 *J. Am. Chem. Soc.* **127** 10806
Kong J, Chapline M and Dai H 2001 *Adv. Mater.* **13** 1384
Ye X R *et al* 2004 *J. Mater. Chem.* **14** 908
Tzitzios V *et al* 2006 *Carbon* **44** 848
Veziri Ch M *et al* 2008 *Microporous Mesoporous Mater.* **110** 41
Vermisoglou E C *et al* 2008 *Microporous Mesoporous Mater.* **110** 25
[9] Subramaniam C *et al* 2007 *Phys. Rev. Lett.* **99** 167404
[10] Daniel M C and Astruc D 2004 *Chem. Rev.* **104** 293
[11] Kumar N A *et al* 2009 *Nanotechnology* **20** 225608
[12] Rao C N R and Nath M 2003 *Dalton Trans.* 1
[13] Dai H *et al* 1995 *Nature* **375** 769
[14] Han W Q *et al* 1997 *Science* **277** 1287
[15] Bezryadin A, Lau C N and Tinkham M 2000 *Nature* **404** 971
[16] Zhang Y and Dai H 2000 *Appl. Phys. Lett.* **77** 3015
[17] Zhang Y *et al* 2000 *Chem. Phys. Lett.* **331** 35
[18] Yang C K, Zhao J and Lu J P 2002 *Phys. Rev.* B **66** 041403
[19] Charlier J-C *et al* 2009 *Nanotechnology* **20** 375501
[20] Bahr J L and Tour J M 2002 *J. Mater. Chem.* **12** 1952
[21] Bendiab N *et al* 2008 *Phys. Rev.* B **78** 104108
[22] Giannozzi P *et al* http://www.quantum-espresso.org
[23] Perdew J P, Burke K and Ernzerhof M 1996 *Phys. Rev. Lett.* **77** 3865
[24] Vanderbilt D 1990 *Phys. Rev.* B **41** 7892
[25] Monkhorst H J and Pack J D 1996 *Phys. Rev.* B **13** 5188
[26] Hakkinen H and Landman U 2000 *Phys. Rev.* B **62** R2287
[27] Okada S *et al* 2000 *Phys. Rev.* B **62** 7634
[28] Jo C, Kim C and Lee Y H 2002 *Phys. Rev.* B **65** 035420
[29] Ohnishi H, Kondo Y and Takayanagi K 1998 *Nature* **395** 780
Rodrigues V, Fuhrer T and Ugarte D 2000 *Phys. Rev. Lett.* **85** 4124
Rodrigues V and Ugarte D 2001 *Phys. Rev.* B **63** 073405
[30] Li T and Balbuena P B 2001 *J. Phys. Chem.* B **105** 9943
[31] Perdew J P and Wang Y 1992 *Phys. Rev.* B **45** 13244
[32] Asaduzzaman A Md and Springborg M 2005 *Phys. Rev.* B **72** 165422
[33] Meunier V *et al* 2009 *Nano Lett.* **9** 1487